Structural and mechanical properties of partially unzipped carbon nanotubes

Chun Tang, Wanlin Guo, and Changfeng Chen

Phys. Rev. B **83**, 075410 — Published 8 February 2011

DOI: 10.1103/PhysRevB.83.075410

Structural and mechanical properties of partially unzipped carbon nanotubes

Chun Tang,[1,2,*] Wanlin Guo,[2,†] and Changfeng Chen[1,‡]

[1]*Department of Physics and High Pressure Science and Engineering Center, University of Nevada, Las Vegas, Nevada 89154, USA*

[2]*Institute of Nano Science, Nanjing University of Aeronautics and Astronautics, Nanjing 210016, China*

We report molecular dynamics simulations of structural and mechanical properties of partially unzipped carbon nanotubes. Our results show that in the absence of edge passivation, partially unzipped carbon nanotubes are unstable with rising temperature depending on the geometry of cutting. When the length-to-width ratio of the graphene segment is not sufficiently large, the dangling bonds at the cutting front tend to reconnect to each other and form back to carbon nanotube structure; otherwise the structures roll up at the graphene end due to the competition of bending stiffness between longitudinal direction and transverse direction. When the graphene edges are hydrogen saturated, the self-healing behavior is suppressed. Tensile tests show that partially unzipped carbon nanotubes exhibit brittle fracture behavior, with a Young's modulus around 700 GPa, which is comparable to that of carbon nanotubes and graphene.

PACS numbers: 61.46.Fg,62.25.-g,64.70.Nd
Keywords: carbon nanotube, unzip, stability, elastic

I. INTRODUCTION

Following the discovery of carbon nanotubes (CNTs)[1], graphene[2] has become another wonder form of carbon materials due to its excellent electronic, mechanical and magnetic properties[3,4]. Methods to synthesize graphene nano ribbons (GNRs) with well defined geometry have been explored[5,6]. Recently, several groups reported benchmark results of producing GNRs from longitudinal unzipping of CNTs[7–11]. The resultant GNRs show promise for applications in nano-electronic devices. Interestingly, besides the desired GNR structures, an unexpected byproduct of incompletely unzipped structures are also found in some experiments[9,10]. Theoretical calculations[12,13] show that such unexpected structures have extraordinary electronic and magnetic properties because this junction structure combines the unique physical properties of CNTs and GNRs. Among the fundamental questions concerning these recently synthesized composite structures is their structural stability and the mechanical properties that are critical to their potential device applications.

In this work, we explore the structural and mechanical properties of the partially unzipped CNTs (PUCNTs) using molecular dynamics (MD) simulations. We find that when the edge dangling bonds are not passivated, PUCNTs show diverse structural transformation behaviors at ambient temperatures. Under most simulation conditions, dangling bonds tend to rebond, leading the structure back to the original CNT pattern, and the speed of such self-healing increases with rising temperature. However, in cases when the cutting length is sufficiently large or the diameter of the original tube is small, the unzipped graphene end rolls up and forms various patterns, which is in good agreement with recent experimental observations[14,15]. When the dangling bonds are passivated with hydrogen atoms, we observe the same rolling up trend with rising temperature. We also studied the tensile properties of PUCNTs. Our simulation results show that PUCNTs exhibit brittle fracture mode at room temperature, with a Young's modulus around 700 GPa, which is comparable to that of CNTs and GNRs. Edge saturation states have no obvious impact on the elastic response under tension.

II. METHODS

The molecular dynamics simulations are carried out using the second-generation Tersoff-Brenner empirical bond-order potential (REBO)[16,17]. It was developed for hydrocarbons on the basis of Tersoff-Brenner expression and the L-J potential in the form of

$$V(r_{ij}) = 4\varepsilon[(\frac{\sigma}{r_{ij}})^{12} - (\frac{\sigma}{r_{ij}})^{6}]$$

describing long range van der Waals interaction was also included[16,17], here the L-J constant used in our simulation are $\varepsilon = 51.2K$ and $\sigma = 2.28\mathring{A}$. This method has been widely used in studies of CNTs and produced key insights for understanding deformation under various loading conditions, nonlinear elastic scaling behavior, and enhanced mechanical properties[18–24]. In particular, it is proven to be accurate in describing bonding-debonding process of

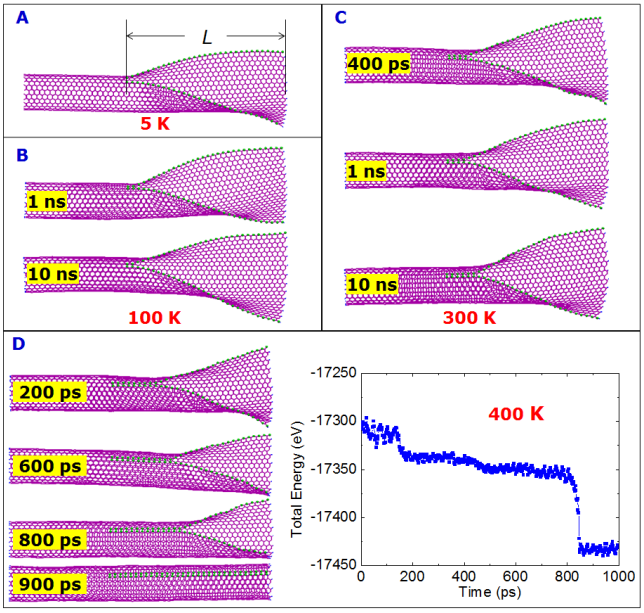

FIG. 1: (Color online) Partially unzipped (12,12) CNT relaxed at different temperatures. Temperatures in panel A to D are 5 K, 100 K, 300 K and 400 K, respectively. Cutting length L=7.4 nm. Also shown in the right panel of (D) is the total energy versus simulation time at 400 K. Carbon atoms at the cutting edges of GNR are highlighted.

carbon materials[25–27], which is key to the process explored in the present study. It should be noted that, however, this method has deficiency in describing fracture mode of carbon nanomaterials at large tensile strain[28,29] although the energetics at low strain levels are reasonable. The Berendsen thermal scheme[30] was employed to control temperature in the simulations. Most of the PUCNTs are obtained by longitudinally cutting one row of C-C bonds and relax the structure at near zero temperature.

III. RESULTS AND DISCUSSION

Experimentally, the unzipping process can be realized through oxidation[7], plasma etching[8], intercalation[9], functionalization combined with STM manipulation[10] or electrical unwrapping[11]. PUCNTs are mainly observed in the intercalation experiment[9] or functionalization[10], and in the former approach, mass conservation is maintained during the unzipping process. Also, it is noticed that bare edge states have been observed by several experiments[31,32]. We therefore focus on the structures obtained by a "cutting" method, i.e. we longitudinally cut one row of C-C bonds and then investigate their structural and mechanical properties. In this situation, the edge atoms with dangling bonds may not be sufficiently saturated by functional groups or hydrogen. We therefore mostly consider structures without hydrogen passivation and show that the dangling edge states lead to rich new phenomena. We also examine structures with different edge states and those obtained from different unzipping method.

A. Structural properties of partially unzipped CNTs

Fig.1 presents a series of results for a partially unzipped (12,12) single-walled CNT (SWCNT), where the unzipping length L along the axis direction in this model is 7.4 nm. It can be seen that at low temperature (for example, at T=5K), partially unzipped SWCNTs are stable, the dangling bonds at the cutting edge show no reconstruction as observed in flat graphene nano sheets or GNRs[33–35]. However, when we heat the system to higher temperatures, the edge dangling bonds lose their stability. Unlike the reconstruction behavior frequently observed in GNR edges[33–35], the unsaturated carbon atoms at the cutting front reconnect to each other, and the whole structure thus self-heals back to the original CNT geometry. This is because dangling bond states have higher energy [see Fig. 1(D)], approximately 4 eV for each pair of dangling bonds from our calculation, consistent with results of Koskinen *et al.*[34]. In addition, at the junction area between the CNT and GNR segments, strong local stress exists since the C-C bond length in the CNT segment is elongated (the C-C bond length at the cutting crack front is 1.446 Å). This 1.8% elongation leads

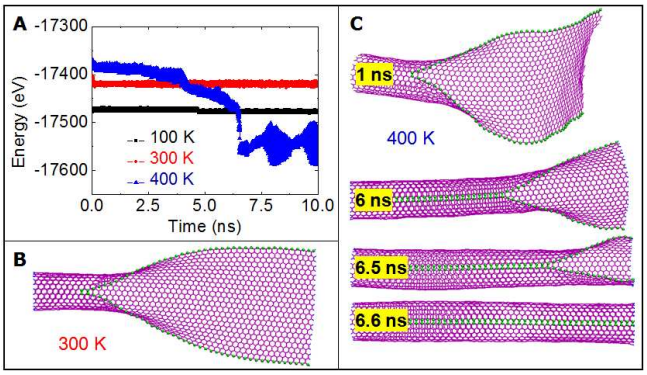

FIG. 2: (Color online) Structural evolution of partially unzipped (12,12) CNT relaxed at different temperatures. A: Total energy versus time in the simulation, some snapshots at 300 K and 400 K are given in B and C. The cutting length in this model is 10.4 nm.

to a pulling force of 2.8 eV/Å, slightly larger than the edge stress of bare GNRs[36]. These two driving forces together with thermal energy therefore pulls dangling atoms at the edges of the graphene segment back towards each other; thus the unzipping front of the PUCNT tends to roll back to circular shape at sufficient temperature.

We examined this behavior at a series of temperatures up to 400 K. It can be seen from Fig.1 that the self-healing speed increases with rising temperature. At 100 K, two pairs of dangling bonds were found to reconnect after 2 ns simulation; while at 300 K, six pairs self-healed within the same simulation duration. At temperatures above room temperature up to 400 K, due to the increased thermal energy, we find the whole structure self-healed within 900 ps. These pairs of dangling bonds reconnect to each other step by step, leading to the gradual reduction of total energy and eventually reaching its energy minimum at 820 ps. The sharp drop of total energy before the structure completely self-healed indicates that the self-healing speed is not a constant because when approaching the end of self-healing process, the geometry at the crack front is different from flat GNR structure, leading to reduced bending stiffness.

It is noticed that in the experiments[9,10], the system size and the unzipping length are larger than those in our simulations. To conduct simulations at the same scale is beyond current computational capability. We instead studied a series of PUCNTs with different original CNT sizes and cutting lengths to explore the general trend of structural dynamics. We first examine the unzipping length effect. We show in Fig. 2 the results of a (12,12) PUCNT which has longer cutting length (10.4 nm) than that (7.4 nm) in Fig. 1, which yields a larger aspect ratio of the GNR segment. As a result, the flat GNR geometry provides stronger tensile force at the unzipping front (the C-C bond length at the unzipping front increases to 1.46 Å), it therefore tends to prevent the PUCNT structure from self-healing as discussed above. At 100 K and 300 K, our simulations for 10 ns duration show that the PUCNT remains nearly unchanged, only two pairs of dangling bonds reconnected at 300 K [see Fig. 2(b)]. When temperature increases to 400 K, the self-healing process speeds up; however, it is still far slower than the results shown in Fig. 1: here 6.6 ns are required to complete the self-healing process. These results suggest that at low temperatures, larger unzipping length can enhance the stability of PUCNTs, thus impeding the process of rolling back to CNT structures. After the structure rolls back to a SWCNT structure at 400 K, a notable fluctuation in total energy is observed, which can be attributed to the thermally induced resonant behavior of the tube.

Results in Fig.3 show a general decreasing trend of healing rate against cutting length. This behavior can be attributed to the bending stiffness of the unzipped GNR segment[36], $K = Et^3d/12(1-\nu^2)$, where E is the Young's modulus, t the thickness of graphene, d the width and ν the poisson's ratio. The unzipped GNR segment has two primary folding directions: wrapping around the longitudinal axis [$K_l = Et^3l/12(1-\nu^2)$ where l is length of the flat GNR segment, smaller than L] and the transverse axis [$K_t = Et^3d/12(1-\nu^2)$]. Therefore, with increasing unzipping length, K_l gradually increases. Once K_l exceeds K_t, the GNR segment tends to roll up at sufficiently high temperatures, as seen in Fig.2(C). This process plays a key role in slowing the self-healing speed as shown in Fig.3. At further increased l, the rolling of the GNR plays a dominant role in the dynamical process. It is noted (see Fig.3) that the PUCNT with cutting length of 4.3 nm has much higher self-healing rate of 215 nm/ns, which is consistent with the behavior seen in Fig.1(D) and Fig.2(A) where the healing rates become faster at the end of the process. This is because when the cutting length is very short, K_l is almost diminished while K_t increases significantly because it has a geometry in-between GNR and CNT, and the bending stiffness of a CNT [$K_{CNT} = (\pi/8)Etd^3$] is 2-3 orders higher than GNR[36].

In most of our simulations, increasing temperature accelerates the self-healing rates. We however observe one exception for the (12,12) PUCNT with a cut length of 6.2 nm. Its healing rate at 400 K is slightly lower than that at 300 K. This is attributed to the thermal energy induced strong oscillation in transverse direction, which is a process

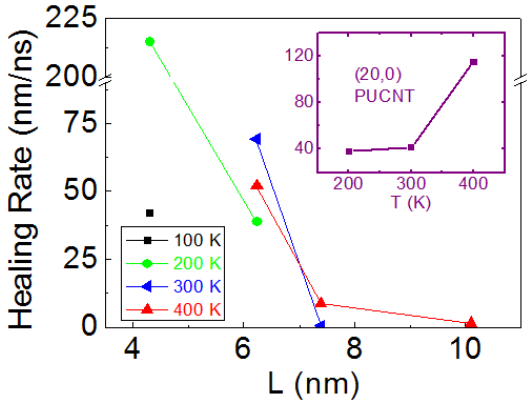

FIG. 3: (Color online)Cutting width dependent healing rate of a (12,12) PUCNT. Inset presents the healing rate of a (20,0) PUCNT versus temperature.

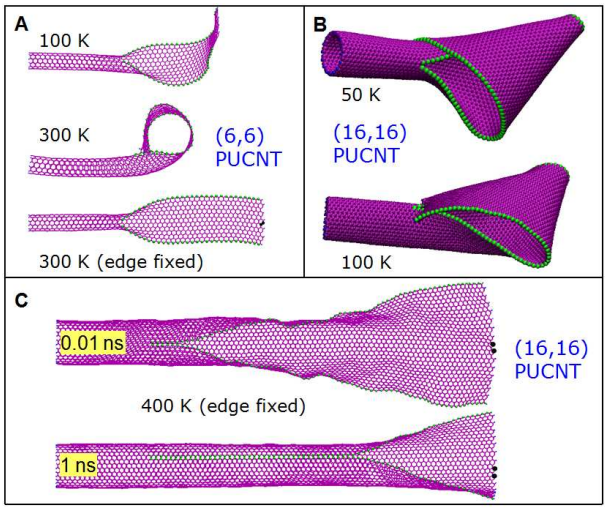

FIG. 4: (Color online) (A): Partially unzipped (6,6) CNTs relaxed at different temperatures; (B): Freestanding (16,16) PUCNT relaxed at 50 K and 100 K; C: Edge fixed (16,16) PUCNT relaxed at 400 K. The fixed atoms in panel A and C are highlighted in Black.

that costs more kinetic energy than in other similar simulations. In all other cases we studied, including zigzag PUCNTs, the conclusion remains unchanged. An example is shown in the inset in Fig.3 presents the temperature dependent healing rate of a (20,0) PUCNT simulated at different temperatures. Due to the different edge state of the GNR segment from that of armchair PUCNTs (the number of dangling bonds is approximately doubled), the healing speed is slightly slower than the corresponding values for armchair PUCNTs. However, the self-healing behavior and its temperature and cutting length dependence remain similar.

The above analysis and evidence shown in Fig.2(C) suggest that for free standing PUCNTs, when the unzipping segment is sufficiently long, $K_l \gg K_t$, the flexible GNR segment should be easier to be bent than zipped, which thereby impedes the self-healing process. Our simulations show that this scenario is typical as shown in Fig. 4. It is seen that unlike the aforementioned self-healing behavior, the (6,6) PUCNT (with a l/d ratio of 3) folds up from the unzipping end, in agreement with that observed in recent experiments[14,15]. With increasing temperature, the degree of folding at the GNR ends becomes stronger. At 300 K, the GNR end completely folds up, forming another tubular structure. Similar behaviors are also observed in the (16,16) PUCNT, which has a cutting length of 17 nm. Due to the folding effect, the self-healing of dangling bonds at the unzipping front is significantly suppressed although the edge dangling bonds are not passivated with hydrogen or functional groups.

To separate the folding effect on the self-healing behavior, we also performed simulation with the GNR ends fixed. For the unzipped (6,6) SWCNT, we still do not see any rebonding process for any dangling atoms. This indicates that for small unzipped CNTs, the intrinsic strain energy[20,37] that comes from the rolling of GNRs to SWCNTs is dominant over the energy gains from the rebonding process and, therefore, rolling back to SWCNT structure is

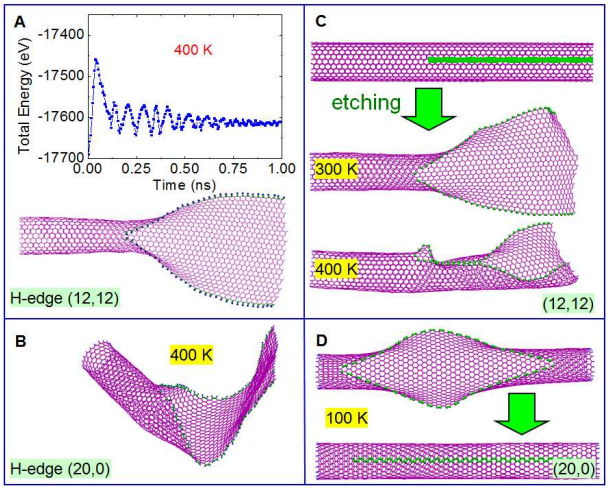

FIG. 5: (Color online) Edge state effect on the stability of partially unzipped CNTs. The edge atoms in PUCNT in (A) and (B) are saturated by hydrogen atoms. The PUCNT structure in (C) is obtained by etching one row of carbon atoms along the axis direction, as sketched in the top CNT structure.

energetically less favorable for small GNRs. While for larger diameter (16,16) PUCNT with long cutting length, when the GNR end is fixed, the lower intrinsic strain energy has much less effect on the re-bonding process and, we again observed the self-healing behavior at 400 K. This reinforces the pivotal role of the competition between the two aforementioned bending stiffness terms since one of the bending freedom (K_t) is prohibited here.

As discussed above and reported in the literature[33,34,38], dangling bonds at the GNR edge are reactive. Hence in device applications at ambient conditions, functional groups or chemical species are likely to attach to the GNR edges. In this situation, the structural dynamics may be notably affected. To simplify the calculation, we saturated the edge atoms with hydrogen atoms as usually treated in theoretical calculations. Results in Fig. 5(A) show that when the (12,12) PUCNT edges are passivated by hydrogen atoms, the PUCNTs completely lose their self-healing ability even when temperature is raised up to 400 K. For the hydrogen saturated (20,0) PUCNT in Fig. 5(B), we also do not observe self-healing behavior. Instead, it is seen that the GNR edge folds up when relaxed at 400 K, similar to the results shown in Fig. 4. Further increase of temperatures (up to 1,000 K) still does not lead to the self-healing behavior, but makes the structure strongly curled.

In addition to the structures discussed above, PUCNTs can also be obtained by etching. In this situation, the distance between the opposite edges of the GNR segment is larger than those obtained by "cutting" method, hence the self-healing ability should be reduced. This is demonstrated by our simulations as shown in Fig. 5(C). Here we remove one row of carbon chains to obtain the partially unzipped structure. When this structure is heated to 300 K, no self-healing behavior is observed. When the temperature is further increased to 400 K, a few dangling carbon atom pairs reconnect to each other. But because the local stress at the junction area is much less, the rebonding process therefore does not start from the SWCNT-GNR junction area as seen in previous results. This suggests that in order to obtain high quality GNR products, chemical etching methods should be a primary choice because they tend to impede the self-healing process by the larger separation of opposite edges. They also provide a more conducive chemical environment for edge state functionalization.

Another class of PUCNT structure is that unzipped from the middle of the SWCNTs while tubular structures at both ends are retained, forming a SWCNT-GNR-SWCNT heterostrucutre. In this situation, the bending stiffness K_t is also suppressed, similar to the situation of edge fixed (16,16) PUCNT shown in Fig.4(C), hence the GNR only has one possible axis to roll up, i.e. the SWCNT axis. Additionally, there are two SWCNT-GNR junctions, hence the self-healing behavior would start from both sides of the GNR, resulting in a faster self-healing process. Our simulations of a (20,0) PUCNT with the middle part unzipped show that it can be self-healed within 0.1 ns at temperature of 100 K, as shown in Fig. 5(D).

B. Elastic properties of partially unzipped CNTs

Elastic properties of PUCNTs are of broad interest since high mechanical strength is one of the key characteristics of CNTs and GNRs. Fig. 6 shows a PUCNT from a (12,12) SWCNT stretched at 300 K, at a strain rate of $0.08\mathring{A}$/5,000fs. The strain energy and stress versus strain curves show typical brittle fracture behavior for the PUCNT: past the elastic

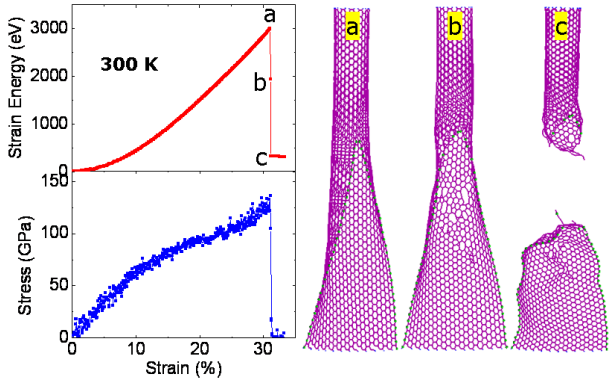

FIG. 6: (Color online) Tensile properties of a partially unzipped (12,12) CNT at 300 K. Left panels show the strain dependent strain energy and stress, typical structural patterns under tension are presented in the right panel. The cutting length in this simulation is 7.4 nm.

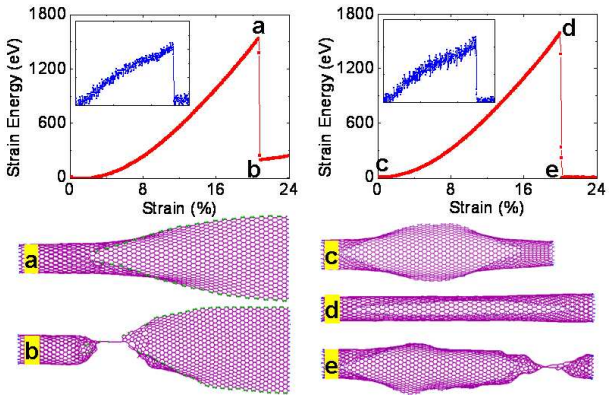

FIG. 7: (Color online) Tensile properties of a partially unzipped (20,0) CNT with different unzipping geometry, insets show corresponding stress *vs* strain curve. The edge atoms of the GNR segment in the right panel are saturated with hydrogen atoms.

limit, the strain energy drops abruptly from 3000 eV to around 320 eV, while the stress decreases to zero, in good agreement with previously reported results on CNTs and GNR[41,42]. The snapshots of the structure during stretching clearly demonstrate the brittle fracture pattern. It is interesting to see that the broken site locates at the junction area that links the CNT and the GNR segments. We find that in all our tensile tests, this fracture mode remains universal. This can be understood from the fact that both the CNT and the GNR segments are seamlessly well-defined one-dimensional structures, while the junction segment can be regarded as either a defective CNT or defective GNR, and it hence has lower tensile strength and breaks prior to the elastic limit of the corresponding CNT or GNR structures. The Young's modulus estimated from our calculation is about 700 GPa, which is comparable to those of CNTs[39] and graphene[40], suggesting that partially unzipped CNTs maintain very good strength, which bodes well for their applications in nano-composites and electromechanical devices.

We now examine the tensile deformation behavior of a zigzag (20,0) PUCNT. Results in Fig. 7 show similar patterns compared to those from armchair (12,12) PUNCT presented in Fig.6. However, the (20,0) PUCNT has a much lower elastic limit of 19.4%. This is because the bond angles of different chiralities have distinct contributions to the elastic stretch: for the armchair PUCNTs or CNTs, the bond angles along the axial direction have larger space to deform, thus leading to higher elastic limit. Our tensile results on GNR structures with armchair and zigzag edges show similar trends as shown in Fig. 8, which is in good agreement with the direct measurement of bond angles of GNRs[42]. It should be noted here, however, that the REBO potential is known to have flaws regarding fracture behaviors of carbon systems under tension due to its overestimation of C-C bond strength over 1.7$\mathring{A}$. Therefore the snapshots in Fig.8(c) and (j) might contain some artificial effects. While other results on elastic moduli and the brittle fracture mode presented in Figs.6 and 7 are expected to be less influenced by this factor. In addition, deriving carbon atomic chains from graphene has been observed in recent experiments[43], which is consistent with our results shown in Fig.8(k).

It is interesting to note that the strain-free GNR structures in our simulations show intrinsic rippling behavior with

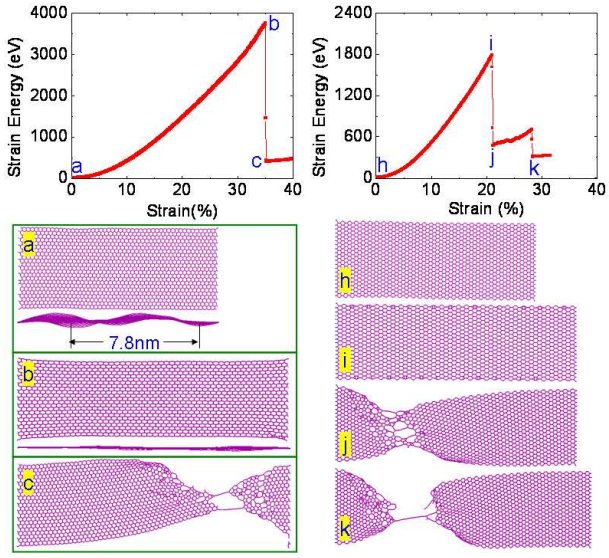

FIG. 8: (Color online) Tensile properties of graphene nano-ribbons obtained by unzipping the (12,12) and (20,0) SWCNTs. Also shown in (a-b) are the side view of the unzipped GNR from (12,12) CNT with intrinsic rippling vanished at large strain.

a typical wavelength of 7.8 nm, which is in agreement with previous observations[44]. However, when tensile strain is applied to the sample, the rippling is effectively suppressed, as shown in Fig. 8(b), resulting in an ultra-flat graphene structure. This result suggests a practical route to graphene structure engineering aiming at using ultra-flat graphene for exploring true two-dimensional physics[45].

We also examined hydrogen saturation effect on tensile behaviors of PUCNTs. The results show no noticeable difference from those of bare edge structures. Both the elastic limits and the fracture patterns remain essentially the same as discussed above. PUCNTs which are unzipped in the middle section of SWCNTs are also examined, as shown in the right panel of Fig. 7. To eliminate the strong self-healing effect in this structure, the edges of the unzipped GNR part are saturated with hydrogen atoms. We again obtain similar results as discussed above. The structure breaks at one of the junction areas between SWCNT and GNR segments.

Another interesting topic is the high temperature elastic properties, we have conducted tensile simulations at 400 K for both armchair and zigzag PUCNTs. The (12,12) PUCNTs show the same behavior as at room temperature, while tests on the (20,0) PUCNTs yield a few topological defects past the elastic limit, suggesting possible tensile ductility at higher temperatures. As high temperature superelongation has been reported both experimentally[46] and theoretically[19], it may be interesting to further investigate whether similar structural deformation patterns exist in PUCNTs at high temperatures up to 2,000 K.

IV. CONCLUDING REMARKS

In summary, we have explored the stability and mechanical properties of partially unzipped CNTs using molecular dynamics simulations. Our results indicate that most bare edge PUCNTs tend to self-heal back to SWCNTs structure at ambient temperatures due to the high reactivity of dangling bonds and local stress at the junction area. PUCNTs with large length or narrow GNR width may fold up at the GNR ends due to the competition of bending stiffness in different directions, in agreement with recent experimental observations. PUCNTs lose the self-healing ability when the edges are saturated by hydrogen atoms. Tensile tests reveal that PUCNTs show brittle fracture mode at room temperature, and the broken sites are located at the junction area of SWCNTs and unzipped GNRs. PUCNTs unzipped from armchair SWCNTs have higher elastic limit than that from unzipped zigzag SWCNTs, in accord with the results of CNTs and graphene. We estimate that PUCNTs have a Young's modulus of about 700 GPa, which is comparable to that of CNTs and graphene. The results presented in this paper provide a useful guide and reference for possible applications of PUCNTs in novel electromechanical devices or nano-composite fibers.

Acknowledgments

Work supported by DOE Cooperative Agreement DE-FC52-06NA26274 at UNLV and 973 Program (2007CB936204), NSF (10732040) of China at NUAA.

---

* Electronic address: tangchun@physics.unlv.edu
† Electronic address: wlguo@nuaa.edu.cn
‡ Electronic address: chen@physics.unlv.edu

[1] S. Iijima, Nature **354**, 56 (1991).
[2] K. Novoselov, A. Geim, S. Morozov, D. Jiang, Y. Zhang, S. Dubonos, I. Grigorieva, and A. Firsov, Science **306**, 666 (2000).
[3] A. Geim, and K. Novoselov, Nature Mater. **6**, 183 (2007).
[4] A. Castro Neto, F. Guinea, N. Peres, K. Novoselov, and A. Geim, Rev. Mod. Phys. **81**, 109 (2009).
[5] X. Li, X. Wang, L. Zhang, S. Lee, and H. Dai, Science **319**, 1229 (2008).
[6] J. Cai, P. Ruffieux, R. Jaafar, M. Bieri, T. Braun, S. Blankenburg, M. Muoth, A. P. Seitsonen, M. Saleh, X. Feng, K. Mllen, and R. Fasel, Nature **466**, 470 (2010).
[7] D. Kosynkin, A. Higginbotham, A. Sinitskii, J. Lomeda, A. Dimiev, B. Price, and J. Tour, Nature **458**, 872 (2009).
[8] L. Jiao, L. Zhang, X. Wang, G. Diankov, and H. Dai, Nature **458**, 877 (2009).
[9] A. Cano-Marquez, G. Rodriguez-Macias, J. Campos-Delgado, C. Espinosa-Gonzalez, F. Tristan-Lopez, D. Ramirez-Gonzalez, D. Cullen, D. Smith, M. Rerrones, and Y. Vega-Cantu, Nano Lett. **9**, 1527 (2009).
[10] M. C. Paiva, W. Xu, M. F. Proenca, R. Novais, E. Lægsgaard, and F. Besenbacher, Nano Lett. **10**, 1764 (2010).
[11] K. Kim, A. Sussman, and A. Zettl, ACS Nano **4**, 1362 (2010).
[12] H. Santos, L. Chico, and L. Brey, Phys. Rev. Lett. **103**, 086801 (2009).
[13] B. Huang, Y. Son, G. Kim, W. Duan, and J. Ihm, J. Am. Chem. Soc. **131**, 17919 (2009).
[14] J. C. Meyer, A. K. Geim, M. I. Katsnelson, K. S. Novoselov, T. J. Booth, and S. Roth, Nature, **446**, 60 (2007).
[15] Z. Liu, K. Suenaga, P. J. Harris, and S. Iijima, Phys. Rev. Lett. **102**, 015501 (2009).
[16] D. W. Brenner, Phys. Rev. B **42**, 9458 (1990).
[17] D. W. Brenner, S. A. Shenderova, J. A. Harisson, S. J. Stuart, B. Ni, and S. B. Sinnott, J. Phys.: Condens. Matter **14**, 783 (2002).
[18] J. Elliott, J. Sandler, A. Windle, R. Young, and M. Shaffer, Phys. Rev. Lett. **92**, 095501 (2004).
[19] C. Tang, W. L. Guo, and C. F. Chen, Phys. Rev. Lett. **100**, 175501 (2008).
[20] C. Tang, W. L. Guo, and C. F. Chen, Phys. Rev. B **79**, 155436 (2009).
[21] A. Kutana and K. Giapis, Phys. Rev. Lett. **97**, 245501 (2006).
[22] X. Li, W. Yang and B. Liu, Phys. Rev. Lett. **98**, 205502 (2007).
[23] B. Peng, M. Locascio, P. Zapol, S. Li, S. Mielke, G. Schatz and H. Espinosa, Nature Nanotech. **3**, 626 (2008).
[24] I. Arias and M. Arroyo, Phys. Rev. Lett. **100**, 085503 (2008).
[25] W. L. Guo, C. Zhu, T. Yu, C. Woo, B. Zhang and Y. Dai, Phys. Rev. Lett. **91**, 125501 (2003).
[26] R. S. Kumara, M. G. Pravicaa, A. L. Corneliusa, M. F. Nicola, M. Y. Hub and P. C. Chowb, Diamond Relat. Mater. **16**, 1250 (2007).
[27] Z. Wang, Y. Zhao, K. Tait, X. Liao, D. Schiferl, C. Zha, R. T. Downs, J. Qian, Y. Zhu, and T. Shen, Proc. Natl. Acad. Sci. USA, **101**, 13699 (2004).
[28] N. Marks, N. Cooper, D. McKenzie, D. McCulloch, P. Bath, and S. Russo, Phys. Rev. B **65**, 075411 (2002).
[29] L. Pastewka, P. Pou, R Prez, P. Gumbsch, and M. Moseler, Phys. Rev. B **78**, 161402 (2008).
[30] H. Berendsen, J. Postma, W. Gunsteren, A. DiNola and J. Haak J. Chem. Phys. **81**, 3684 (1984).
[31] C. Girit, J.C. Meyer, R. Erni, M.D. Rossell, C. Kisielowski, L. Yang, C.H. Park, M. F. Crommie, M.L. Cohen, S.G. Louie, and A. Zettl, Science **323**, 1705 (2009).
[32] X. Jia, M. Hofmann, V. Meunier, B. G. Sumpter, J. Campos-Delgado, J. Romo-Herrera, H. Son, Y. Hsieh, A. Reina, J. Kong, M. Terrones, and M. S. Dresselhaus, Science **323**, 1701 (2009).
[33] B. Huang, M. Liu, N. Su, J. Wu, W. Duan, B. Gu, and F. Liu, Phys. Rev. Lett. **102**, 166404 (2009).
[34] P. Koskinen, S. Malola, and H. Hakkinen, Phys. Rev. Lett. **101**, 115502 (2008).
[35] P. Koskinen, S. Malola, and H. Hakkinen, Phys. Rev. B **80**, 073401 (2009).
[36] K. B. Bets, and B. I. Yakobson, Nano Res. **2**, 161 (2009).
[37] D. H. Robertson, D. W. Brenner, and J. W. Mintmire, Phys. Rev. B **45**, 12592 (1992).
[38] X. Wang, X. Li, L. Zhang, Y. Yoon, P. K. Weber, H. Wang, J. Guo, and H. Dai, Science **324**, 768 (2009).
[39] M. Yu, O. Lourie, M. Dyer, K. Moloni, T. Kelly, and R. Ruoff, Science **287**, 637 (2000).
[40] C. Lee, X. Wei, J. W. Kysar and J. Hone, Science **321**, 385 (2008).
[41] T. Belytschko, S. P. Xiao, G. C. Schatz and R. S. Ruoff, Phys. Rev. B **65**, 235430 (2002).
[42] H. Zhao, K. Min, and N. R. Aluru, Nano Lett. **9**, 3012 (2009).
[43] C. H. Jin, H. P. Lan, L. M. Peng, K. Suenaga, and S. Iijima, Phys. Rev. Lett. **102**, 205501 (2009).
[44] A. Fasolino, J. Los, and M. Katsnelson, Nature Mater. **6**, 858 (2007).
[45] C. Lui, L. Liu, K. Mak, G. Flynn, and T. F. Heinz, Nature **462**, 339 (2009).

[46] J.Y. Huang, S. Chen, Z. Q. Wang, K. Kempa, Y. M. Wang. S. H. Jo, G. Chen, M. S. Dresselhaus and Z. F. Ren, Nature **439**, 281 (2006).